Oxidative degradation of 2-ethanolamine; the effect of oxygen concentration and temperature on product formation

Solrun Johanne Vevelstad[a], Andreas Grimstvedt[b], Jørund Elnan[a], Eirik Falck da Silva[b] and Hallvard F. Svendsen[a]*

[a]*Norwegian University of Science and Technology, 7491 Trondheim, Norway*
[b] *SINTEF Materials and Chemistry, 7465 Trondheim, Norway*
**Corresponding author: Tel.: +47 73594100 E-mail adress:* hallvard.svendsen@chemeng.ntnu.no

Abstract
Oxidative degradation experiments on 2-ethanolamine (MEA) were performed at four different oxygen concentrations and at two temperatures. MEA loss and degradation product build-up were measured. Increasing the temperature from 55 to 75 °C was shown to have higher impact on the MEA loss than increasing the oxygen concentration from 21 to 98%. Liquid end sample analyses were performed for all experiments and overall nitrogen balance tests were conducted for the experiments at 21% O_2 (run 2), 50% O_2 and 98% O_2. Analysis of liquid and gas phase ammonia and MEA in the solvent was found to give a good overall picture of degradation in the MEA system. The degradation products formed at the different oxygen concentrations were the same as described in earlier literature. However, it was found that oxygen affects the formation of the individual degradation products differently. At 75°C the development of degradation product concentrations with time was more complex. Laboratory reaction experiments were used to verify the formation of certain degradation products from some of the suggested mechanisms.

Keywords: 2-ethanolamine; oxidative degradation; degradation compounds; mechanism; nitrogen balance

1. Introduction

Post-combustion CO_2 capture by absorption is currently the most mature technology for CCS and can be applied both for retrofit and Greenfield plants. Chemical absorption has been widely used for natural gas sweetening for over 60 years. The best absorbents combine high net cyclic capacity, equilibrium temperature sensitivity and reaction/absorption rates for CO_2, good chemical stability, low vapour pressure and low corrosiveness. The most common alkanolamines studied are 2-ethanolamine (MEA), diethanolamine (DEA), *N*-methyldiethanolamine (MDEA), 2-amino-2-methylpropanol (AMP) and blends of these and other amine promoters like Piperazine.

Degradation in reactive absorption systems may occur thermally with CO_2 present or through oxidative degradation, depending on the conditions. Thermal degradation has been studied by several research groups over a long period of time (Davis and Rochelle, 2009; Eide-Haugmo, 2011; Lepaumier et al., 2009a; Polderman et al., 1955) while oxidative degradation has received increased attention the last decade (Goff and Rochelle, 2004; Lepaumier et al., 2009; Rooney et al., 1998; Supap et al., 2001) as it was discovered that oxidative degradation compounds are the main products under real plant conditions (da Silva et al., 2012; Lepaumier et al., 2011a; Strazisar et al., 2003). Increased insight into the degradation mechanisms, through knowledge of stoichiometry, kinetics, and chemical pathways, may result in methods for eliminating or strongly reducing degradation. The oxidative degradation experiments described in the literature are mainly performed in a variation of two setups.

Either the amine loss was studied working in a closed-batch reactor at elevated temperatures and oxygen pressures (Lepaumier et al., 2009; Supap et al., 2001; Wang and Jens, 2011), or in an open-batch reactor at 55 °C where the CO_2-loaded amine solution would be sparged with a wet gas blend of CO_2 and air (da Silva et al., 2012; Goff and Rochelle, 2004; Lepaumier et al., 2011a; Lepaumier et al., 2011b). Lately there has been increased focus on the effect of temperature swing under industrial operation and an integrated solvent degradation apparatus (ISDA) was developed where the solvent is exposed to both oxidative and thermal degradation conditions in a single system (Closmann and Rochelle, 2011). Over the years several oxidative degradation experiments were performed by researchers studying different aspects of degradation like overall degradation rate (Blachly and Ravner, 1966; Chi and Rochelle, 2002), degradation products formed (da Silva et al., 2012; Lepaumier et al., 2009; Sexton and Rochelle, 2011; Supap et al., 2006), stability of the amines (Kohl and Nielsen, 1997; Lepaumier et al., 2009; Rooney et al., 1998) and the effects of oxidation catalyst (Goff and Rochelle, 2006), CO_2 loading (Bello and Idem, 2006; Chi and Rochelle, 2002; Lawal et al., 2005; Rooney et al., 1998; Supap et al., 2009; Uyanga and Idem, 2007), inhibitors (Chi and Rochelle, 2002; Goff and Rochelle, 2006), amine and oxygen concentration (Bello and Idem, 2006; Goff and Rochelle, 2004; Supap et al., 2009; Uyanga and Idem, 2007), agitation rate (Goff and Rochelle, 2004), temperature (Bello and Idem, 2006; Lawal et al., 2005; Supap et al., 2009; Supap et al., 2001). The overall degradation rate was often determined by monitoring the evolution of NH_3 (Chi and Rochelle, 2002) or a combination of NH_3 and peroxide (Blachly and Ravner, 1966).

Oxidative degradation compounds can be separated into primary and secondary products, where primary products are the initial compounds formed such as aldehydes, carboxylic acids and ammonia. The primary degradation compounds are formed by either electron or hydrogen abstraction mechanisms (ammonia, aldehyde) or oxidation products of some of these compounds (acids). The initial mechanisms are still unclear, but the general impression is that the mechanisms either start with abstraction of an electron from the lone pair of nitrogen or abstraction of hydrogen from the nitrogen, α-carbon, or β-carbon, or a combination of these depending on the amine structure, nature of oxidants, pH, solvent effects and concentrations (Bedell, 2009; Chi and Rochelle, 2002; Goff and Rochelle, 2004, 2006; Hull et al., 1967; Hull et al., 1969; Rosenblatt et al., 1967; Sexton, 2008)

Secondary degradation compounds are formed by reactions between primary degradation compounds and amines forming for example amides as *N*-(2-hydroxyethyl)-formamide (HEF), *N*-(2-hydroxyethyl)-acetamide (HEA) and *N*,*N*'-Bis(2-hydroxyethyl)-oxamide (BHEOX) from MEA and acid, or aldehyde and oxygen, and imidazoles as *N*-(2-hydroxyethyl)imidazole (HEI) from ammonia, MEA and several aldehydes. Lately several mechanisms have been suggested for the formation of secondary degradation compounds (da Silva et al., 2012; Lepaumier et al., 2011a; Strazisar et al., 2003). However, there are still many unanswered questions regarding factors influencing the formation of these degradation compounds.

The present paper describes results from oxidative degradation experiments in a laboratory scale open setup at different oxygen concentrations and at different temperatures. The overall nitrogen balance together with the nitrogen balance for liquid phase is given. In addition it is shown how temperature and oxygen concentration influence the formation mechanism of especially secondary degradation products. This can also shed more light on the formation of primary degradation products.

2. Experimental section

The amine used was 2-ethanolamine, MEA [141-43-5] (Sigma-Aldrich, purity > 99%).

Amine solution (30 wt%) was prepared gravimetrically using distilled water. A loading of 0.4 mol CO_2 per mol amine was maintained in the experiments and produced by bubbling CO_2 gas through the solution until the desired weight was obtained. Actual amine concentrations were measured using LC-MS and amine titration, and CO_2 concentrations were measured for the start and end samples using the $BaCl_2$ method (Ma'mun et al., 2007). In addition selected samples were analysed for metals (ICP-MS), nitrogen (Kjeldahl method) (Kjeldahl, 1883), density, anions (IC), alkylamines and ammonia (GC-MS/LC-MS), nitrosamine (LS-MS-MS-QQQ) and other degradation compounds shown in the supporting information.

Oxidative degradation setup

Open batch setup

The amine solution (MEA), loaded with CO_2 (α= 0.4 mol CO_2 per mol of amine), was introduced into an open batch reactor (1L) according to the flow sheet shown in Figure 1.

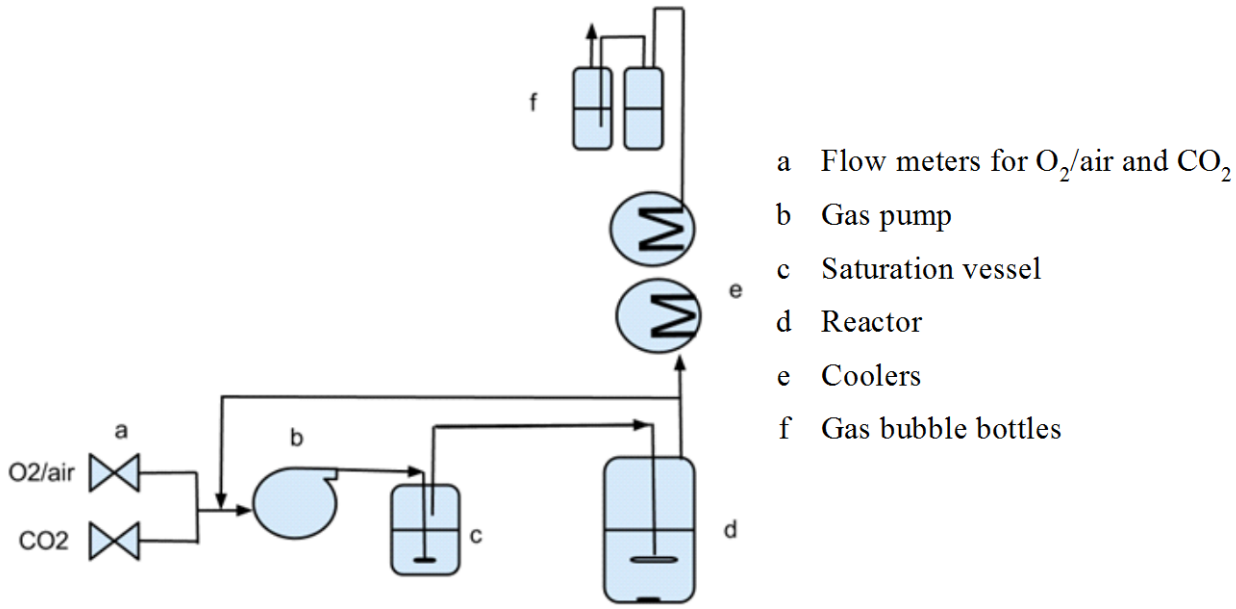

Figure 1: Flowsheet for open batch setup.

Na_2SO_4 (10-30 mM) was added to the solution to have a control for the water balance during the experiments. A recycle loop maintained a circulation rate of about 50 L/h of a gas blend of air/O_2 with 2% CO_2. The gas was humidified by passing through a contactor c and sparged into the solution in reactor d and a net throughput of gas was obtained by adding (0.35 L/min air/[98%O_2]/[50%O_2+50%N_2] + 7.5 mL/min CO_2) to the recycle loop. The reactor temperature was maintained at 55 °C or 75 °C. The exhaust gas was bubbled through gas bubble flasks containing water or 0.05 M H_2SO_4 as shown in the flow sheet. Samples were taken regularly from the liquid phase and the gas bubble flasks and analysed by the analytical techniques mentioned above. All the concentrations were reconciled according to the water balance.

Mixing experiments

Specific experiments were performed to investigate the formation of *N*-(2-hydroxyethyl)-imidazole (HEI) and 2-[(2-hydroxyethyl)amino]-2-oxo-acetic acid (HEOX) from possible intermediates. The experiments were conducted with MEA in excess (factor of 3-9 times on mole basis). For the experiments with more than one reactant in addition to MEA, the reactants (except MEA) were found in 1:1 molar ratio. The specific tests were:

For HEI

1) MEA, ammonia, formaldehyde and glyoxal:
MEA (5.0 g) and ammonia (1.34 g of a 25 wt% aqueous solution) were mixed together and heated to 60 ºC. Glyoxal (2.6 g of a 40 wt% aqueous solution) and formaldehyde (1.4 g of a 36.5 wt% aqueous solution) were mixed together to a homogenous solution and then added drop-wise to the mix of MEA and ammonia, which turned yellow. The resulting aqueous solution containing MEA (48 wt%), ammonia (3 wt%), glyoxal (10 wt%) and formaldehyde (5 wt%) was stirred at 60 °C for 5 hours.

2) MEA, formaldehyde and oxamic acid:
MEA (5.3 g), oxamic acid (1.1 g) and formaldehyde (1.2 g of 36.5 wt% aqueous solution) were mixed together. The resulting aqueous solution of MEA (69 wt%), formaldehyde (6 wt%) and oxamic acid (15 wt%) was heated to 50-60 °C and stirred for 6.5 hours. After 30 minutes, a white solid appeared in the mix.

For HEOX

1) MEA and oxalic acid:
Oxalic acid (15.0 g, 28 wt%) was weighed out, MEA (38.3 g, 72 wt%) was slowly added under stirring. The solution was stirred at room temperature for 1 hour before the solution was stirred at 55 °C for 4.5 hours.

2) MEA and oxamic acid:
Part 1: MEA (98.8 g, 87 wt%) was added to oxamic acid (14.8 g, 13 wt%). The solution was stirred at 55 °C for 5.5 hours.
Part 2: The product from part 1 was reacted with NaOH (5 M, 35 mL), heated to approximately 55 °C and stirred for 6 hours.

Analyses

Several analytical methods were used and quantification was conducted for the compounds given in table 1.

Table 1: Compounds quantified using different analytical methods: LC-MS, GC-MS or IC-anion.

Abbreviation	Compound	CAS	Structure	Analytical method
BHEOX	*N,N'*-Bis(2-hydroxyethyl)-oxamide	1871-89-2	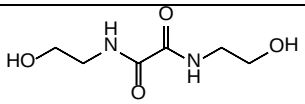	LC-MS ("LC-MS mix")
HEA	*N*-(2-hydroxyethyl)-acetamide	142-26-7	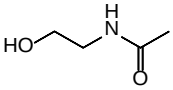	LC-MS ("LC-MS mix")
HEF	*N*-(2-hydroxyethyl)-formamide	693-06-1	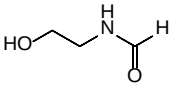	LC-MS ("LC-MS mix")
HEGly	*N*-(2-hydroxyethyl)-glycine	5835-28-9	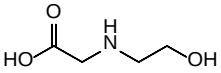	LC-MS ("LC-MS mix")
HEI	*N*-(2-hydroxyethyl)-imidazole	1615-14-1	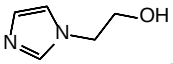	LC-MS ("LC-MS mix")
HEPO	4-(2-hydroxyethyl)-2-piperazinone	23936-04-1	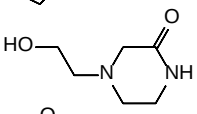	LC-MS ("LC-MS mix")
OZD	2-Oxazolidinone	497-25-6	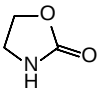	LC-MS ("LC-MS mix")
DEA	Diethanolamine		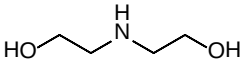	LC-MS
	Formate		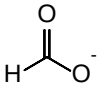	IC-anion
	Nitrite		NO_2	IC-anion
	Nitrate		NO_3	IC-anion
	Oxalate		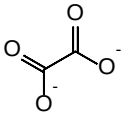	IC-anion
	Ammonia	7664-41-7	NH_3	GC-MS or LC-MS
MA	Methylamine	74-89-5		GC-MS or LC-MS
DMA	Dimethylamine	124-40-3	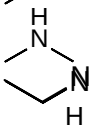	GC-MS or LC-MS
EA	Ethylamine	75-04-7		GC-MS or LC-MS
DiEA	Diethylamine	109-89-7	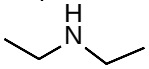	GC-MS or LC-MS

Ion Chromatography (IC)

The samples were diluted in deionized water (18.2 MΩ) and analysed for formate, acetate, glycolate, oxalate, nitrite and nitrate (IC-mix) on an ICS-5000 Dual RFIC Ion Chromatography Dionex System. The system was equipped with two different columns: IonPac AG15 guard column (2*50 mm)/AS15 analytical column (2*250 mm) or IonPac AG11HC guard column (2*50 mm)/AS11-HC analytical column (2*250 mm). In addition the system contains an ASRS300 suppressor (2 mm), a carbonate removal device (CRD-200, 2 mm) which removes carbonate from the degraded sample, a continuously regenerated anion trap column (CR-ATC) which removes carbonate from the eluent and a CD conductivity detector. The system uses an EG eluent Generator Module with a potassium hydroxide eluent generator cartridge. The eluent generator is connected to an ICW-3000 water purification system (Millipore system). A gradient method with potassium hydroxide was used as eluent, starting either on 1 mM or 6 mM KOH depending on the column, both ending at 60 mM KOH.

All standards used for calibration were purchased from Sigma Aldrich with purity higher than 97%. All the degraded samples were diluted in deionized water (18.2 MΩ). The level of

dilution depended on column, type of analysis and level of degradation and anion analysed. For almost all experiment several dilutions were used and an average value used when possible.

LC-MS/GC-MS

Liquid Chromatography–Mass Spectrometry (LC-MS) was used to determine the amine concentration (mol/L) and the concentration of degradation products; "LC-MS mix" (HEI, HEF, HEA, BHEOX, OZD, HEGly and HEPO), ammonia and alkylamine (table 1) in the degraded samples. The start and end samples from the experiment at 21% O_2 at different temperatures were in addition analysed in full scan mode to detect degradation products not yet a part of the degradation mix analysed for. The system used was an LC–MS/MS 6460 Triple Quadrupole Mass Spectrometer coupled with a 1290 Infinity LC Chromatograph and Infinity Autosampler 1200 Series G4226A from the supplier Agilent Technologies. The molecules were converted to ions using electrospray ionisation (ESI) for "LC-MS mix", amine, full scan mode, ammonia and alkylamine analysis. The analytical column for amine and scan analyses was an Ascentis Express RP- Amide HPLC Column (15cm x 4.6 mm,2.7µm, Cat#:53931-U, Supelco Analytical, Bellefonte, USA), while a Discovery HS_F5 column (15cm x 4.6mm, 3µm, Cat#:567507-U, Supelco Analytical, Bellefonte, USA) was used for the degradation compounds in the LC-MS mix. The MEA quantification was performed diluting the samples 1/10000 in water and adding an internal standard (MEA d_4 – $HO\text{-}CD_2\text{-}CD_2\text{-}NH_2$). The internal standard made it possible to correct for drift in the instrument and matrix. The initial sample for full scan analysis was diluted 1/100 in water for positive scan ($M+H^+$) and 1/100 for negative scan ($M\text{-}H^+$). The full scan analysis may in addition give MS-fragments and adducts like $M\text{-}Na^+$ for the same molecule depending on the conditions used. Dilution for the quantification of the LC-MS-mix was 1/10000 in water. More details around calibration can be found in the supporting information in the publication by da Silva (da Silva et al., 2012). Mobile phase for amine and full scan mode was 25mM formic acid + methanol in gradient. Ammonium acetate (0.1 %) and methanol were used for the LC-MS mix.

GC-MS was in addition used to measure contents of ammonia and volatile alkylamines using derivatisation for experiment no. 1 (MEA run 1). Dansyl chloride was used as derivatisation reagent. For the remaining experiments an LC-MS method was developed, also using derivatisation with 5-(dibutylamino)-1-naphthalenesulfonyl chloride for DMA and dansyl chloride for ammonia and the rest of the alkylamines. Ascentis Express C18 (15cm x 2.1mm, 2.7µm, Cat#:53825-U, Supelco Analytical, Bellefonte, USA) was used for the LC-MS analysis of ammonia and alkylamine. The quantification of ammonia and alkylamine were performed by diluting the samples in water and adding deuterated internal standards. The mobile phase was 25 mM formic acid + acetonitrile in gradient.

GC-MS was also used to identify some degradation compounds for the 21% O_2 MEA 55 °C, system and method as described by Lepaumier (Lepaumier et al., 2011b).

Inductively coupled plasma spectroscopy – mass spectroscopy (ICP-MS)

The initial and end samples for each experiment in the open batch system, where $NaSO_4$ was added for control of the water balance, were in addition analysed for sulphur. This was done using ICP-MS. The instrument used was an Element 2 from Thermo Fisher (Bremen, Germany).

Titration (total alkalinity and CO_2)
The total alkalinity of the solution for the screened systems was determined by acid titration (0.1 M H_2SO_4) using a standard procedure described by Kim (Kim et al., 2008) and the CO_2 concentrations in start and end samples were measured by the $BaCl_2$ method described by Ma'mun (Ma'mun et al., 2007).

Density
The density of the end samples were measured on a Mettler-Toledo CM40 at 22 °C where three parallels were run for each sample.

Total nitrogen
Total nitrogen in the end sample was measured using the Kjeldahl method (Kjeldahl, 1883).

3 Results

MEA stability

Stability of MEA at different conditions in the open setup is illustrated by change in amine concentration (mol/L) over time (days) as seen in Figure 2. It was assumed that an increase of mass during an experiment is caused by water condensation since water saturated gas was used. All concentrations were adjusted according to the water balance, typically 2-4% at 55 °C and ~7% at 75 °C.

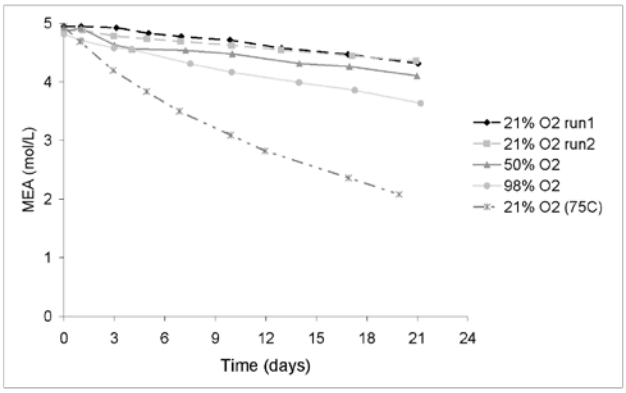

Figure 2: Decline in amine concentration (mol/L) over time (days) for experiments conducted at different temperatures (55 and 75 °C) and oxygen concentrations (21-98%).

For a given oxygen concentration and at 55°C, the amine concentration, as seen in Figure 2, decreases almost linearly with time. At 75°C the curve is not linear as a slight decrease in degradation rate with time is seen. This may be a natural consequence of the degradation rate being a first order function of MEA concentration. At 55°C the degradation is so low that this effect is not seen. The effect of temperature is seen to be very strong. An increase of 20 °C, from 55 to 75°C gave a 4.5 fold decrease in amine concentration (mol/L) after 3 weeks..

Degradation rates (mM/h) for the experiment at 55 °C were found assuming linear behaviour. The degradation rates were then plotted as a function of oxygen concentration in Figure 3. A degradation rate at 6% O_2 (grey triangle) was roughly estimated from a screening oxidative degradation setup and included in Figure 3 (experimental details and information for this experiment are given in supporting information). Three of the 4 experiment in the open batch setup were conducted over a time period of 2 months (the three filled black squares) while the last experiment was conducted 1.5 year earlier (empty square at 21% O_2).

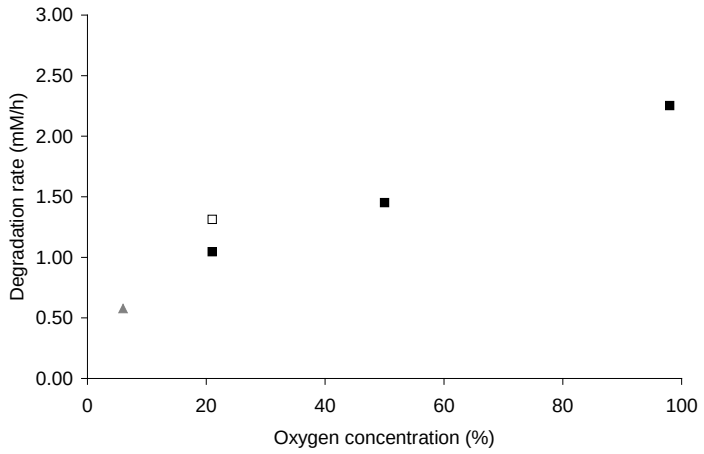

Figure 3: Degradation rate (mM/h) plotted toward oxygen concentration for experiments conducted at 55 °C (oxygen concentration 21-98% from open batch setup (squares, unfilled experiment conducted 1.5 years earlier, 6% from screening setup (grey triangle)).

Figure 3 indicates that there is a linear dependency between degradation rate and oxygen level for oxygen concentrations between 21 and 98% at 55 °C. The number of points is low, however, and should be validated with more oxygen concentrations. Below 21% there seems to be a gradual decrease in the effect of oxygen. This can be due to limitations in oxygen mass transfer which has been suggested by other authors (Goff and Rochelle, 2004).

Supap (Supap et al., 2009) found that the initial degradation rate for runs at 393 K for 100% oxygen concentration was about 28 times higher than the one at 21% oxygen concentration. As comparison the initial degradation rate for the data in this work was calculated using the same method (exponential function) as described by Supap (Supap et al., 2009). The initial degradation rate at 328 K for the run at 98% was 2.3 times higher than the one at 21% oxygen. The experiments (Supap and present paper) were performed in different experimental setups and at different temperatures and CO_2 concentrations which all would influence degradation. Supap (Supap et al., 2009) also found that temperature has a higher impact on the degradation than an increase in oxygen concentration as confirmed by this work. The low gas flow system described by Sexton (Sexton and Rochelle, 2009) is quite similar to the open batch system used in the present work. Assuming linear loss of amine during the duration of the experiment the MEA loss was found to be 2.3 mM/h for the experiment using 98% O_2. As a comparison, Sexton (Sexton and Rochelle, 2009) found, with added iron, a loss of 3.8 mM/h of MEA. Both of the systems are open systems, gas (98% O_2, 2% CO_2) is introduced continuously and both experiments were performed with CO_2 loading (α=0.4). However Sexton (Sexton and Rochelle, 2009) added iron to the experiment. Iron has earlier been found to increase degradation, which could explain the higher loss shown for the experiment performed by Sexton.

Nitrogen balance

The end samples from each experiment were analysed for nitrogen according to the Kjeldahl method (Kjeldahl, 1883). In table 2 is shown how MEA and the sum of known degradation compounds (LC-MS mix and NH_3) contribute to the liquid phase organic nitrogen balance for the end sample. The N unaccounted column is the balance up to 100%. The uncertainty in nitrogen recovery for the experiment at 21% O_2 at 55 °C was found to be 5%. Assumptions, together with the calculations of the uncertainty are given in supporting information.

Table 2: Nitrogen balance for end sample liquid phase.

T (°C)	O_2 (%)	MEA (%)	N in known degradation compounds (%)	Nitrogen recovery (%,R_N)
55	21	89	4	93+/-5
55	21	94	2	96+/-5
55	50	89	3	92+/-5
55	98	82	4	86+/-4
75	21	56	6	62+/-3

The nitrogen containing degradation compounds analysed are seen to account for about the same percentage independently of the oxygen concentration. That there is an unaccounted balance for nitrogen to fill indicates that there are still unknown degradation compounds. The discrepancy in the nitrogen balance increases with oxygen level which indicates that these compounds are influenced by the oxygen concentration. Also there could be new degradation products formed at higher oxygen concentrations.

In Table 3 the formation of degradation products is given. Percentage formation of degradation products ($\tau_{f,i}$) in liquid phase is calculated by the method described by Lepaumier (Lepaumier et al., 2011b) and given by $\tau_{f,i} = \nu_i * \frac{C_i^m}{C_0^m} * 100$

where ν_i is number of nitrogen in the degradation product, C_i^m is the molar concentration of the degradation products and C_0^m is the initial concentration of MEA.

Table 3: Operating conditions for the experiments together with MEA loss and % formation of nitrogen containing degradation compounds in the end sample

Oxygen %	21	21	21	50	98
Temperature, °C	75	55	55	55	55
MEA loss (%)	58	13	11	16	24
			% formation		
OZD	0.22	0.086	0.074	0.14	0.22
BHEOX	0.063	0.068	0.068	0.16	0.22
HEA	0.18	0.015	0.018	0.027	0.041
HEGly	0.20	0.16	0.17	0.18	0.15
HEPO	0.15	0.024	0.024	0.027	0.027
HEF	0.76	0.47	0.88	1.90	1.97
HEI	0.74	0.10	0.099	0.21	0.40
DEA	0.012	0.0048	-	-	0.0037
NH_3 (l)	2.22	3.27[a]	0.19	0.26	1.058
Sum organic N (%)	4.55	4.20	1.52	2.92	4.08
NO_2	0.45	0.10	0.12	0.27	0.32
NO_3	0.22	0.040	0.035	0.093	0.16
Sum inorganic N (%)	0.66	0.14	0.16	0.37	0.48
N unidentified (%)	52.70	8.47	8.90	12.41	19.94

[a]Analysed by GC-MS, a more uncertain quantification method.

Ammonia and HEF were found to be the main degradation compounds contributing to the nitrogen balance in liquid phase as shown in table 3.

As mentioned earlier the experiments with oxygen concentrations 50 and 98% and MEA run 2 (21%) were all run over a two month period. For these experiments the exit gas was bubbled through sulphuric acid (0.05M) to measure the ammonia and MEA content in the outlet gas. The analyses showed that the acid concentration in the gas bubble flask was too low and that the maximum capture capacity was reached after between 4 and 14 days for these experiments. The total nitrogen in table 4 was calculated by adding the nitrogen contributions from the degradation compounds (LC-MS mix, nitrite, nitrate and ammonia, also given in table 4) in the solvent end sample together with the outlet gas contribution from MEA and ammonia divided by the initial amine (mol).

Table 4: Total nitrogen balance (liquid and gas phase) for 3 degradation experiments at different oxygen concentration conducted over a two month period.

Experiment	LC-MS mix (mol)	NO_2&NO_3 (mol)	MEA (mol)		NH_3 (mol)		Total N (%)
	Solvent	Solvent	Solvent	Outlet gas	Solvent	Outlet gas	
21% O_2 run2	0.063	0.0074	4.24	0.0013	0.0092	0.039	88
50% O_2	0.13	0.017	3.88	0.0021	0.013	0.070	85
98% O_2	0.15	0.022	3.57	0.0062	0.051	0.070	78

The end sample liquid concentrations were corrected for gain of water (2-4%). Due to the limited acid concentration in the gas bubble flask the amounts of ammonia and MEA in the outlet gas in table 4 are underestimated. In table 4, it is seen that ammonia is the most

important degradation compound. MEA (in solvent) and ammonia (in solvent and outlet gas) are the main contributors to the nitrogen balance and they can be used to give an overall estimate of the degradation in the system. In total the nitrogen accounted for decreases from 87% at 21% to 77% at 98% oxygen level indicating that more ammonia was lost at the higher oxygen concentrations where the degradation was higher.

The outlet gas for the two other experiments; MEA run 1 and MEA 75 °C, was bubbled through water and the end samples were analysed for MEA and the LC-MS mix degradation compounds. All of the degradation compounds in the LC-MS mix, except BHEOX (boiling point not known), have a boiling point higher than 190 °C and their presence in the outlet gas cannot be explained by volatility. The amount of each compound in the outlet gas were compared toward the end liquid sample and found to be lower than 0.01% at 55 °C and less than 0.1% at 75 °C except for HEF which was less than 1% at 75 °C (more information is found in supporting information). The amount of MEA in the gas bubble flask was estimated from analyses and found to be less than 1% of the MEA loss.

Degradation compounds (liquid phase)

The effect of temperature and oxygen concentration on the formation of different degradation compounds was investigated. The degradation compounds quantitatively determined are given in Table 1 in the experimental part.

Primary degradation compounds

Ammonia and formate are primary degradation compounds formed in significant quantities. Ammonia in liquid phase was analysed using LC-MS or GC-MS ([a]GC-MS for 21% O_2 run 1) and nitrite and nitrate were analysed by IC. Nitrite and nitrate are most likely formed in oxidation reactions between NH_3 and O_2. The concentrations (mmol/L) of ammonia, nitrite and nitrate with time are given in Figure 4.

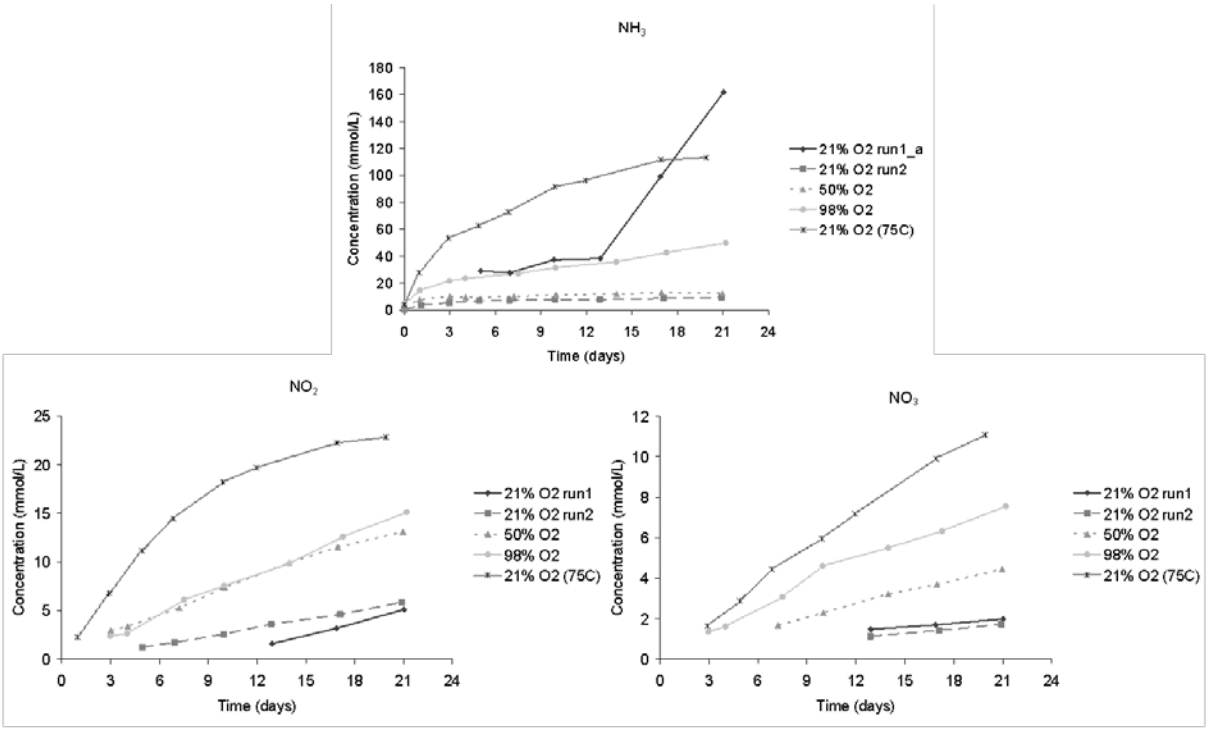

Figure 4: Concentration (mmole/L) of NH_3 , NO_2 and NO_3 as function of time (days) for experiments at different oxygen concentrations and temperatures ([a]ammonia analysed on GC-MS for 21% O_2 run 1)

The relationship between the formation of ammonia, nitrite and nitrate during oxidative degradation of amines is not fully understood. Ammonia is one of the main components in waste waters containing nitrogen and several techniques have been investigated and developed for the oxidation of ammonia (Huang et al., 2008; Wang et al., 1994). Hydroxyl radicals are the primary oxidant in several of these oxidation processes oxidizing ammonia into nitrite and subsequently to nitrate. A detailed mechanism for the oxidation of ammonia with hydroxyl radical in aqueous phase, with hydrogen peroxide as precursor for hydroxyl radical, is suggested by Huang (Huang et al., 2008). Several steps and radicals are believed to be formed resulting in $NH_2O_2^-$ which could dissociate to nitrite. Nitrate is then formed gradually from oxidation of nitrite by hydrogen peroxide or hydroxyl radical.

From Figure 4 the general trend is that the formation of nitrate, nitrite and ammonia all increase with increasing O_2 level. However, in the experiment performed at 50% O_2 nitrite is formed in about the same rate as at 98% O_2. For ammonia the formation at 50% O_2 is about the same as at 21% O_2. This is unexpected but the two observations are consistent with each other. An explanation for this could be that ammonia formation is slower than ammonia oxidation to nitrite going from 21 to 50% oxygen concentration and that the oxygen concentration has less impact on nitrite formation when going from 50 to 98% oxygen. The formation of nitrate is seen to increase with oxygen concentration and also the ratio between NO_3 and NO_2 increases with increasing oxygen concentration. This indicates that the oxidation of NO_2 to NO_3 is more favoured at higher oxygen concentrations as expected. At higher temperature the formation of ammonia increases more than the ammonia oxidation to nitrite and the oxidation to nitrate increases even less. This may be explained by the reactions being consecutive and thus the effect of higher degradation rate is weakened down the chain of reactions. It may also partly be an effect of lower oxygen solubility at higher temperature.

Oxalate and formate are primary degradation products believed to be intermediates in the formation of several secondary degradation compounds as explained in the introduction. It is therefore difficult to isolate the behaviour connected to the formation of these anions from their role in in further reactions. Their concentrations (mmol/L) as function of time are given in Figure 5 and the end sample concentrations as function of oxygen concentration are plotted in Figure 6.

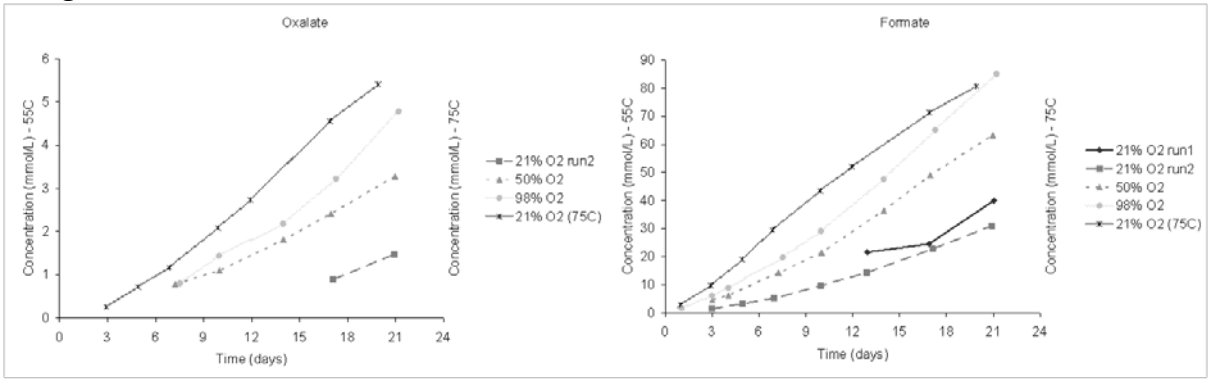

Figure 5: Oxalate and formate concentration (mmol/L) over time (days) for the experiments at different temperatures and oxygen concentrations.

Oxalate and formate formation seem to be close to linear with time. The detection limit for the anions varies between the different experiments because the analytical methods were under continuous development and in addition the levels of dilution necessary were decided for each individual degradation experiment. This can be seen for the experiments at 21% O_2 and 55 °C where samples from run 1 were run at higher dilution, giving higher detection limits than for

run 2. Traces of oxalate were discovered in run 1, but the amount never exceeded the detection limit.

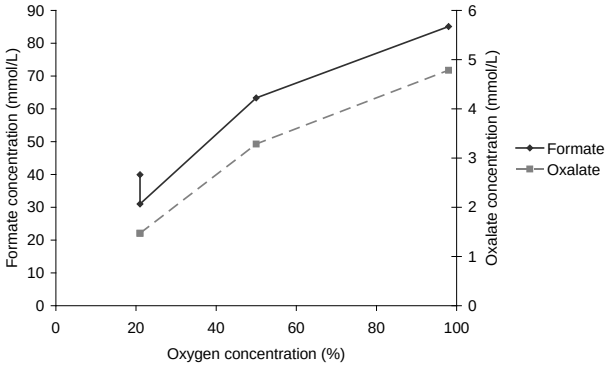

Figure 6: Concentration of formate and oxalate (mmol/L) for the end samples for experiments conducted at 55 °C plotted against oxygen concentration.

Oxalate and formate seem to react similarly to an increase in oxygen concentration as seen in Figure 6. Increase in temperature is seen, Figure 5, to influence formate and oxalate more than oxygen concentration. There are indications that oxalate formation is more influenced by temperature than formate since calculations show that the ratio of formate to oxalate is reduced at higher temperatures. This observation might indicate that oxalate formation to a higher extent is favoured by higher temperature. On the other hand, it has also been reported that oxalic acid can decompose to formic acid and CO_2 (Higgins et al., 1997), and thermal degradation experiments on oxidatively degraded solutions conducted at 135 °C showed that oxalate was reduced already the first week (Vevelstad et al., 2013). However, in the present tests temperature did not exceed 75°C.

Except ammonia, all the primary degradation compounds studied in this paper are analysed by IC. In addition to formate, oxalate, nitrate, nitrite and sulphate (added, see experimental section), a peak (likely to be HEOX) at retention time 9.4 minutes was seen (see Figure 7, end sample 21% O_2 run 2).

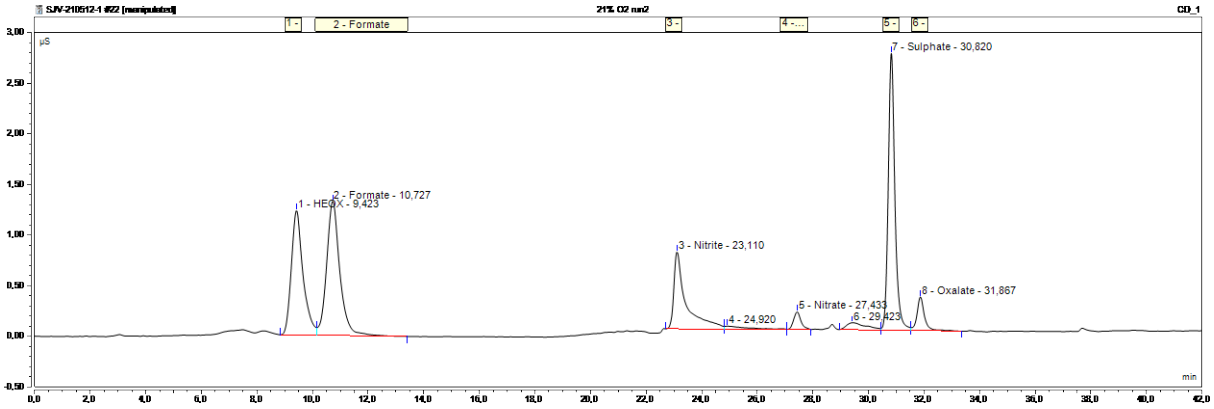

Figure 7: Chromatogram (AS11-HC) for end sample MEA experiment at 21% oxygen run 2.

Formate, nitrite, nitrate, sulphate and oxalate in the chromatogram were identified and quantified using external standards. However a standard for HEOX was not available. In order to support the assumption of a HEOX peak, an experiment was performed where MEA and oxalate were mixed and heated as described in the experimental procedure. Analysing this mixture in the same way as the degradation samples gave the same peak as shown in the

degradation product chromatogram, Figure 7. This was taken as strong support for the peak being HEOX. Acetate and glycolate would have had retention times lower than the HEOX peak if they were present, which they thus are shown not to be.

Secondary degradation compounds

In the following the formation of the various secondary degradation products is given and discussed connected to the concentrations of their primary precursors.

BHEOX, HEF and HEA

BHEOX, HEA and HEF are believed to be formed by condensation reactions between the respective acids, or aldehydes and O_2, and MEA (da Silva et al., 2012). The formation of these compounds as function of time is given in Figure 8.

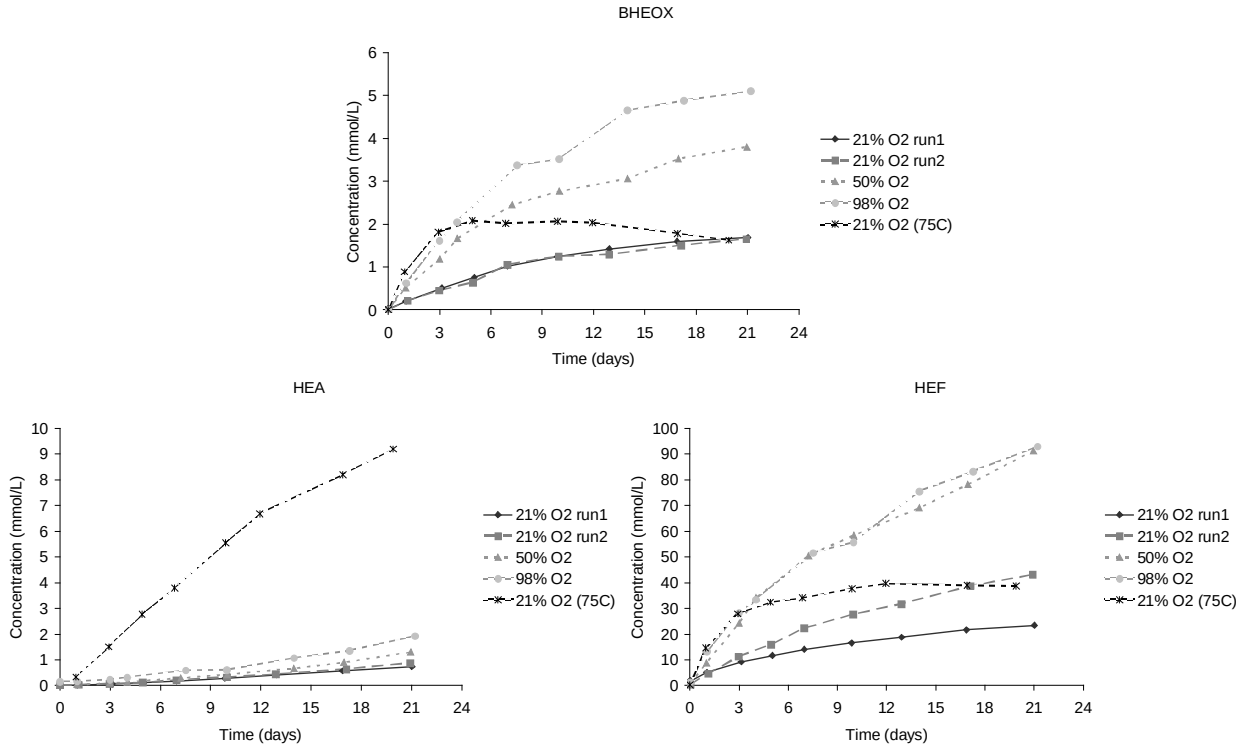

Figure 8: Concentration (mmol/L) of BHEOX, HEF and HEA over time (days) for experiments at different temperatures (55 or 75 °C) and oxygen concentrations (21-98%).

From Figure 8 it is seen that at 55 ^oC the initial rates of formation of BHEOX, HEA and HEF generally increase with increasing oxygen concentration as expected. For HEF, however, the amounts formed as function of time at 50 and 98% are seen to be very similar over the whole duration of the experiment. This trend is not reflected in the amounts of formate formed as seen in Figure 5. The three compounds react differently to temperature. Both the HEF and BHEOX concentrations at 75^oC increase rapidly during the first 5-7 days, but then level off. The BHEOX concentration even decreases. This could point to these compounds being either intermediates for further reaction or being reduced by a back reaction (BHEOX) at higher temperatures. HEA, at 21% O_2 and 55 °C, is the degradation compound in the LC-MS mix formed in the smallest amount. However, the temperature has a very strong effect on the HEA formation and Figure 8 shows that at 75 ^oC the amount of HEA formed is higher than BHEOX. The amount of HEA formed at 75 °C is 18 times higher than at 55 °C for the end sample.

The concentrations of respectively BHEOX and HEF as function of oxygen concentration are shown in Figure 9 together with the data for formate and oxalate.

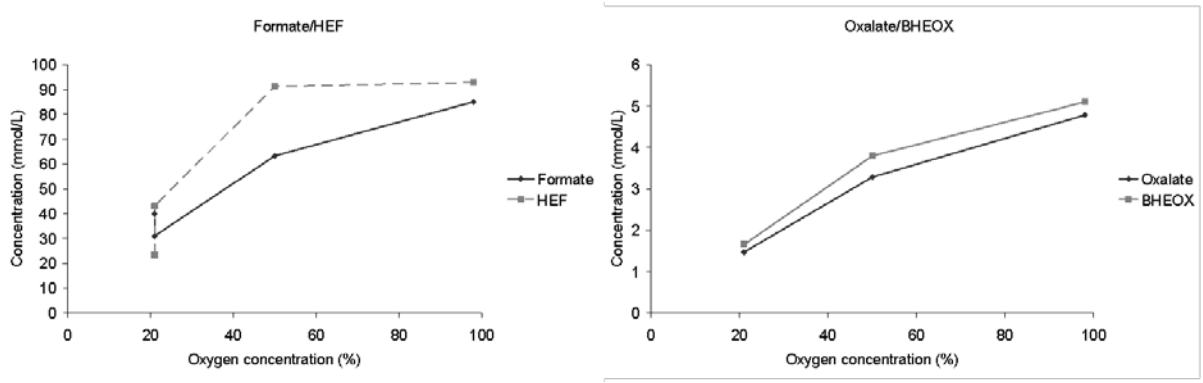

Figure 9: Concentration (mmol/L) of formate, HEF, oxalate and BHEOX for end samples from experiments conducted at 55 °C plotted against oxygen concentration.

From Figure 9 it is seen that the formation of HEF and BHEOX follow their primary probable precursors relatively closely regardless of oxygen concentration. This may indicate that the further formation of the secondary products is relatively fast and possibly governed by equilibrium between respectively oxalate and BHEOX and formate and HEF. Acetic acid was not detected (below detection limit) so the formation of HEA cannot be compared in this way. However, the formation of HEA in measurable quantities indicates that acetic acid or acetaldehyde has been formed. If the same equilibrium assumption is made the implication would be that the reaction from acetic acid/acetaldehyde to HEA is shifted all the way to HEA.

The concentrations of format are of the same order of magnitude as the HEF concentrations and in Figure 10 is shown the HEF/formate molar ratio for the various experiments.

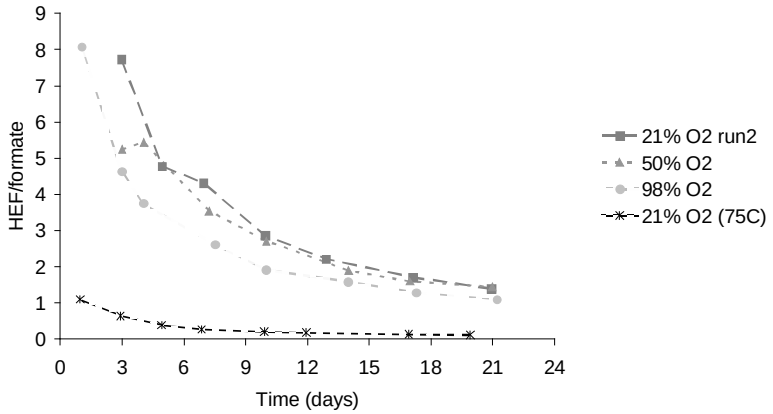

Figure 10: HEF/formate molar ratio for the experiments at different oxygen concentration (21-98%) and temperatures (55-75 °C).

For the tests at 55 ºC it is seen that the curves level off and end up at approximately the same value, regardless of oxygen concentration. This could indicate that an equilibrium or pseudo-equilibrium is reached. Since formate is continuously formed no real equilibrium will be reached. For BHEOX a similar situation is seen in Figure 11.

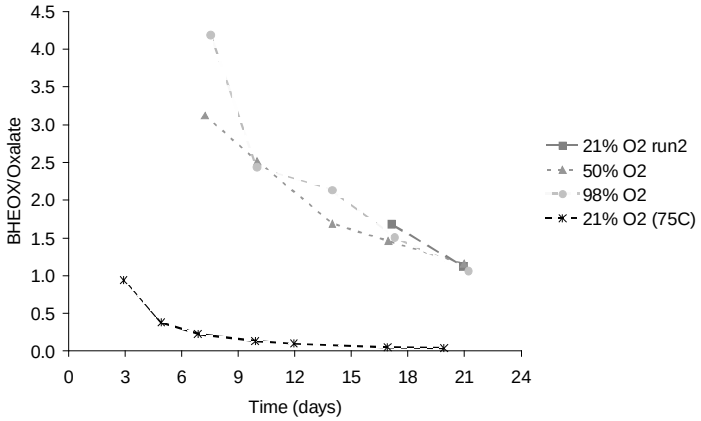

Figure 11: BHEOX/oxalate molar ratio for the experiments at different oxygen concentration (21-98%) and temperatures (55-75 °C).

At 55 ºC the pseudo equilibrium is not established so fast, but also here the equilibrium is shifted toward oxalate at higher temperatures. What may seem non-intuitive is the shape of all the curves showing high HEF/formate and BHEOX/oxalate ratios at the early stages.

HEGly and HEPO

No mechanism has been suggested for the formation of HEGly. On the other hand, HEPO is believed to be formed in a two-step procedure from HEGly and MEA (da Silva et al., 2012), where the first step is a condensation reaction similar to the formation of HEF, BHEOX and HEA, but giving *N*-(2-hydroxyethyl)-2-[(2-hydroxyethyl)amino]-acetamide (HEHEAA). HEHEAA is then cyclised to give HEPO. The formation of these two compounds is given in Figure 12.

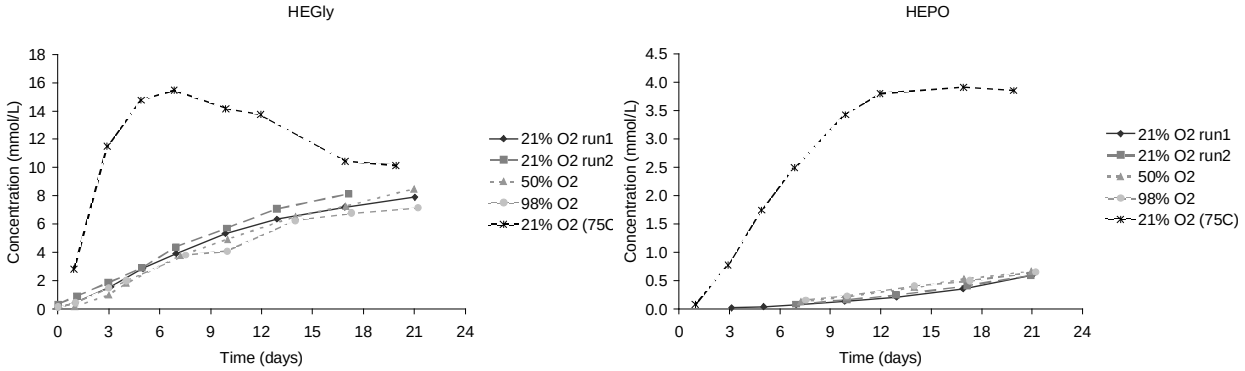

Figure 12: Concentration (mmol/L) of HEGly and HEPO and HEGly over time for MEA experiments at different oxygen concentrations (21-98%) and temperatures (55 and 75 °C),

At 55 ºC neither the formation of HEPO nor HEGly seem to be influenced by the oxygen concentration. The amounts formed are the same for all the oxygen concentrations tested. Temperature is seen to strongly increase both HEGly and HEPO formation rates. At 75 ºC the HEGly concentration peaks after 6 days, however, and then decreases. The decrease in HEGly concentration is consistent with it being a precursor to HEPO which is seen to increase in concentration up to about day 12 whereafter the concentration levels off as less HEGly is available for its formation. Why the HEGly formation rate at 75 ºC peaks at day 6 is not known but the seen behaviour of both HEGly and HEPO at this temperature is supported by lab experiments at higher temperatures (Vevelstad et al., 2013). HEPO and HEGly were found to be the main degradation products in pilot plant samples and it was also suggested

that temperature swing in plants decides the ratio between HEPO and HEGly (da Silva et al., 2012).

HEI

HEI has been reported as an important degradation compound in pilot samples (da Silva et al., 2012). It has also been reported that imidazoles can be synthesised in a one pot synthesis from glyoxal, ammonia and formaldehyde (Prasanthi et al., 2007). Several patents report on the syntheses of different substituted imidazoles. Kawasaki (Kawasaki et al., 1991) and Ben (Ben, 2005) reported formation of HEI from glyoxal, formaldehyde, MEA and ammonia. The concentration (mmol/L) of HEI with time (days) at different oxygen concentrations and temperatures in our experiments is given in Figure 13.

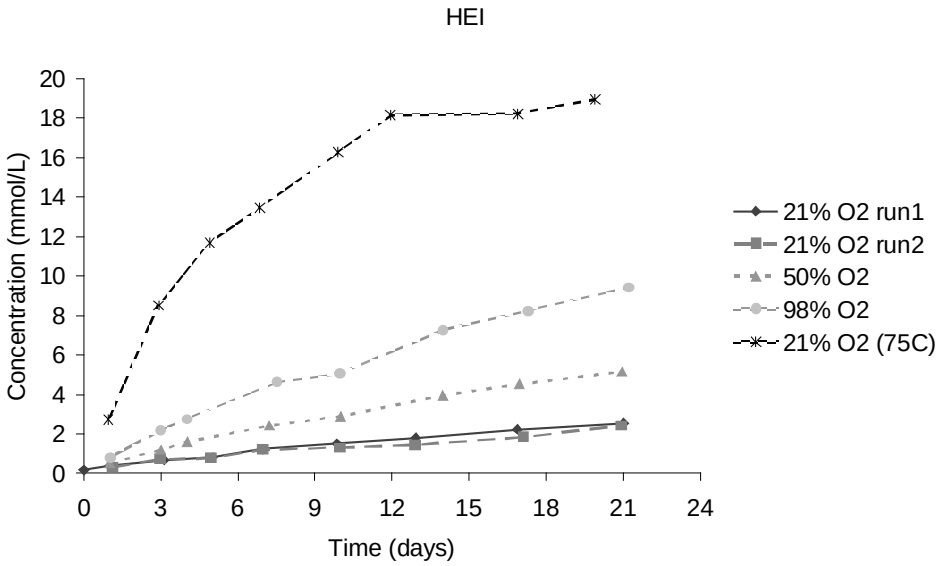

Figure 13: Concentration (mmol/L) of HEI over time for experiments at different temperatures (55 or 75 °C) and oxygen concentrations (21-98%)

HEI formation increases with oxygen concentration and temperature. At 55 ºC there seems to be an almost linear relationship between oxygen content (Figure 14) and HEI formation whereas at 75 ºC the curve seems to follow the behaviour of HEPO, a steeper slope the first 12 days and then levelling off (see Figure 12).

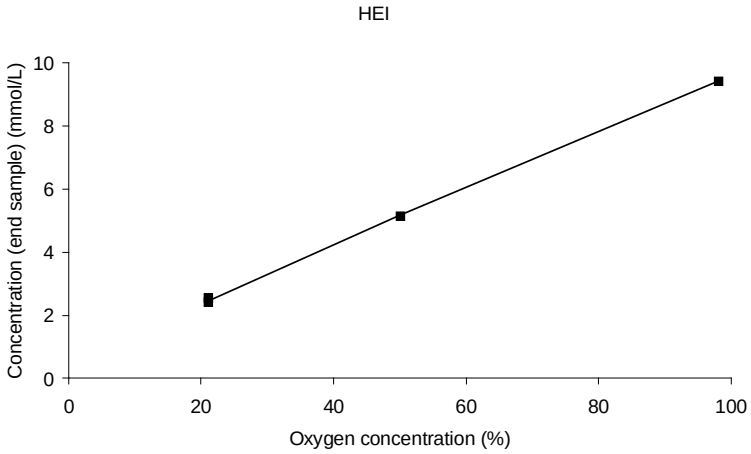

Figure 14: Concentration (mmol/L) of end sample at 55 °C plotted toward oxygen concentration (21-98%)

All of the compounds which Ben (Ben 2005) used to synthesise HEI have been reported as degradation compounds from MEA by several research groups (Gouedard et al., 2012; Sexton and Rochelle, 2011). Literature also reports that the syntheses of different imidazoles take place around 60 or 70-90 °C (Ben, 2005; Prasanthi et al., 2007). Katsuura reports formation of HEI from 2-(methyleneamino)-ethanol and iminoacetaldehyde, where 2-(methyleneamino)-ethanol is formed from MEA and formaldehyde and iminoacetaldehyde from glyoxal and ammonia at 25 °C. The two imines then react to give HEI as suggested in the mechanism given in Figure 15, which is in accordance with Katsuura (Katsuura and Washio, 2005).

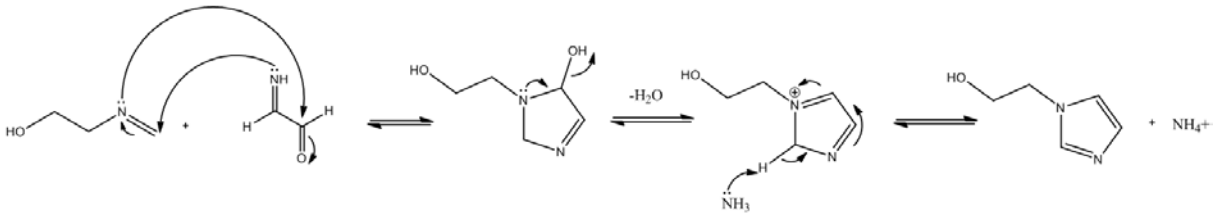

Figure 15: Suggested mechanism for formation of HEI from 2-(methyleneamino)-ethanol and iminoacetaldehyde

HEI formation from glyoxal, formaldehyde, MEA and ammonia was verified in mixing experiments done in this work where MEA and ammonia were mixed, heated to 60 °C and then glyoxal and formaldehyde were added as a homogenous solution drop-wise to the original solution. The experiment was ended after 5 hours. Both GC-MS and LC-MS verified that HEI was present in the solution, in addition a peak at mass to charge ratio (m/z) 74 was found in the positive LC-MS scan (LC-MS full scan positive mode) which could correspond to 2-(methyleneamino)-ethanol. HEI was also found as a by-product when mixing oxamic acid, formaldehyde and MEA (also a peak at m/z 74 was found). LC-MS positive scans from degradation experiments at 55 and 75 °C also showed peaks at m/z 127, 143 and 157, which could be variations of HEI changing formaldehyde to respectively acetaldehyde (Lepaumier et al., 2011a; Rooney et al., 1998; Sexton and Rochelle, 2011; Supap et al., 2006), glycol aldehyde (Goff and Rochelle, 2004; Lepaumier, 2008) or glyoxylic acid (Rooney et al., 1998). These are all suggested products or intermediates for MEA degradation. GC-MS results for the MEA degradation experiments at 55 °C also showed a molecular peak at m/z 126 (see supporting information) and the MS fragmentations were similar to HEI supporting that this compound could be 1-(2-hydroxyethyl)-2-methylimidazole, see Figure 16.

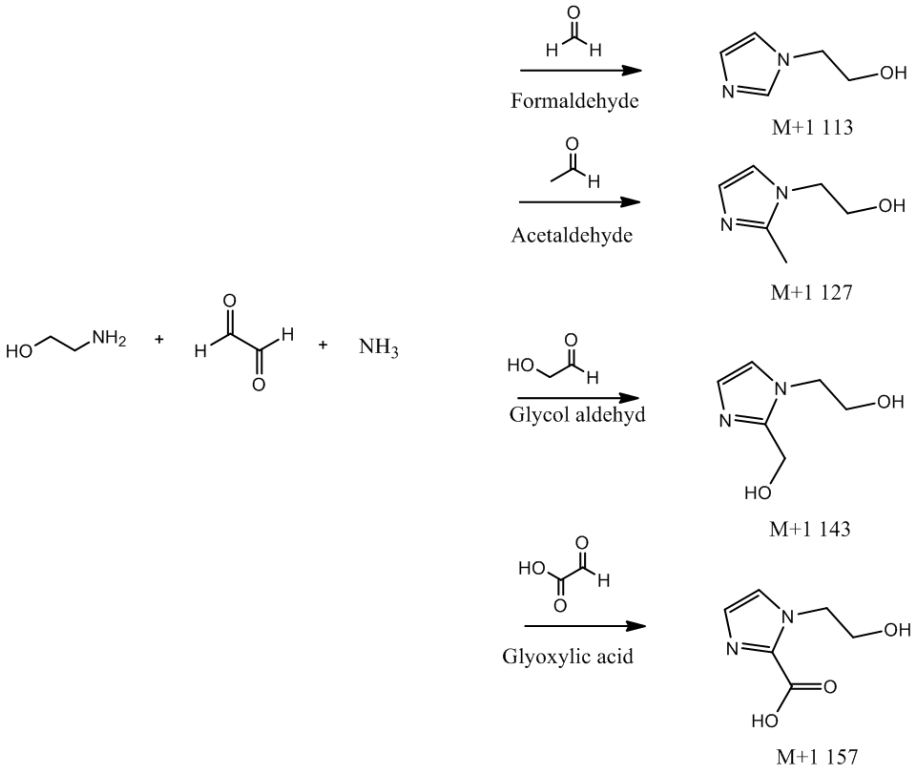

Figure 16: Formation of HEI and possible new degradation products (imidazoles) formed in same type of mechanism as HEI.

However, none of the aldehydes given in Figure 16 were identified in this work because the analytical methods used in this study were not suitable for aldehydes. Thus, further tests have to be performed to verify these compounds. The LC-MS positive scan ($M+H^+$) showed some similar masses when comparing the experiments performed at the two temperatures (55 °C and 75 °C). The results are shown in Figure 17 for m/z 113, 143 and 157 where increase in peak area from initial to end samples is plotted towards the mass ($M+H^+$).

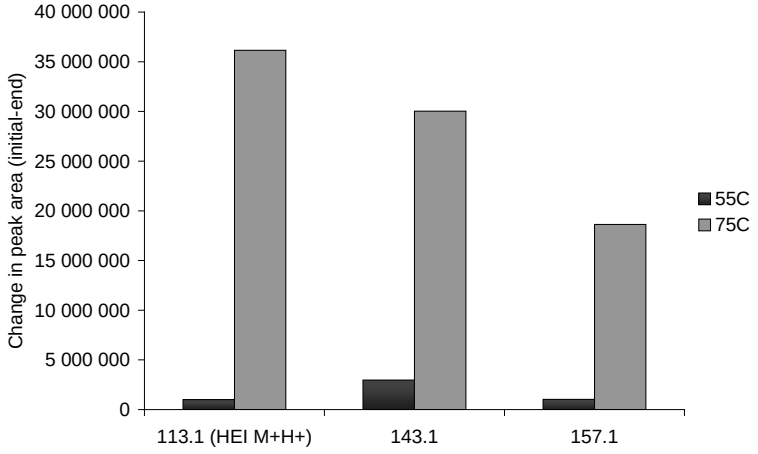

Figure 17: Change in peak area from initial to end sample for some of the common unknown masses from the positive LC-MS scans ($M+H^+$) .

The peaks are believed to be variants of HEI which show a similar behaviour as HEI. An increase in temperature increases the peak area. The peak area (initial-end) at 75 °C for $M+H^+$ 143 was found to be 10 times higher than for the experiment at 55 °C, 18 times higher

for $M+H^+$ 157. As comparison the peak area for HEI was 36 times higher at the higher temperature.

OZD

The concentration (mmol/L) of OZD as function of time is given in Figure 18.

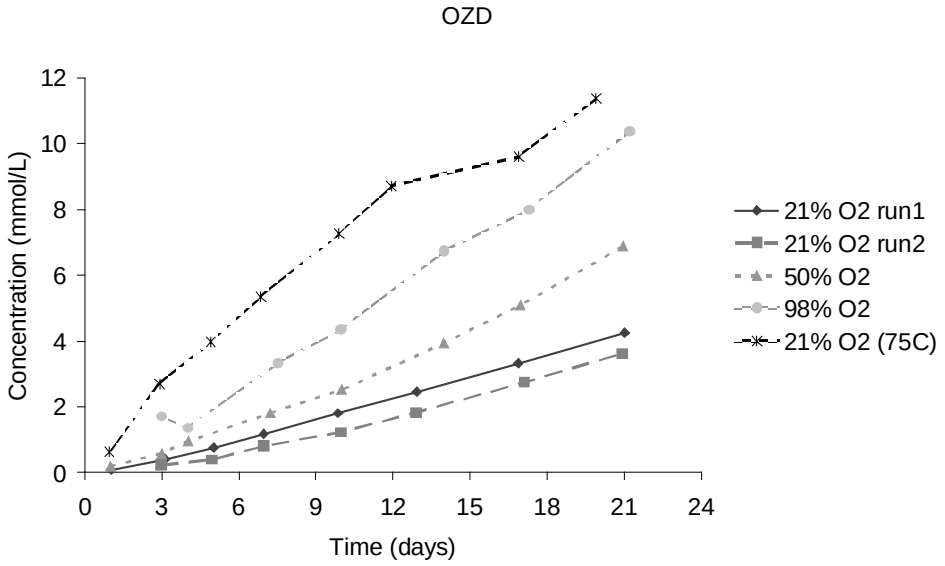

Figure 18: % formation of OZD over time for experiments conducted at different temperatures (55 or 75 °C) and oxygen concentrations (21-98%)

OZD formation increases both with oxygen concentration and temperature. OZD has been observed both in thermal degradation experiments with CO_2 and in oxidative degradation experiments (da Silva et al., 2012). Up to this point it has been assumed that OZD is formed by the same mechanism as for thermal degradation with CO_2, namely by MEA-carbamate ring closure (da Silva et al., 2012). However, it is seen that OZD formation is strongly affected by the oxygen concentration which cannot be accounted for using the suggested mechanism. Patil et al. synthesised OZD in good yields using a phosphonium catalyst in a two-step procedure from epoxides and CO_2, with cyclic carbonates as an intermediate in the reaction given in Figure 19 (Patil et al., 2008). Lepaumier suggested that primary amines, through de-alkylation reactions, could give epoxides (Lepaumier et al., 2009). The mechanism behind the de-amination is not clear but a radical initiated de-amination might explain the seen OZD dependence on oxygen concentration.

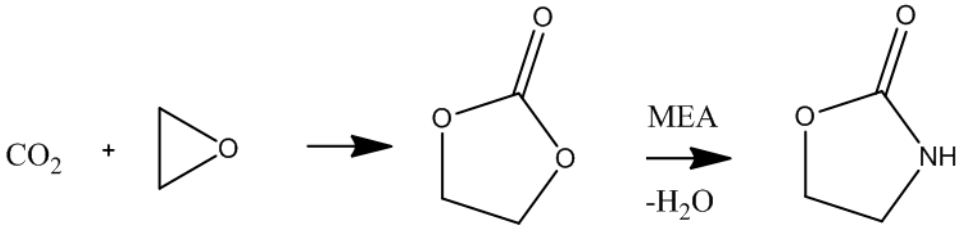

Figure 19: Suggested mechanism for OZD formation under absorber conditions.

4. Conclusions

Oxidative degradation experiments on MEA were performed at four different oxygen concentrations and at two temperatures and MEA loss and degradation product build-up

measured. Increasing the temperature from 55 to 75 °C was shown to have higher impact on the MEA loss than increasing the oxygen concentration from 21 to 98%. Liquid end sample analyses were performed for all experiments and overall nitrogen balances tests were conducted for experiments at 21% O_2 (run 2), 50% O_2 and 98% O_2. At 55^{o}C only 4-14% of the liquid phase organic nitrogen was unaccounted for. Ammonia was found to be the most important degradation compound, and ammonia in the gas and liquid phase and MEA in solvent phase gives a good overall estimate of degradation. At 75 ^{o}C 25% of the liquid phase organic nitrogen was unaccounted for. The degradation products formed at the different oxygen concentrations were the same as described earlier by da Silva (da Silva et al., 2012). However, it was found that oxygen affects the formation of the individual degradation products differently. Almost all degradation products were formed in higher amounts at higher oxygen concentrations, but an exception was found for HEF and NO_2 at 50 and 98% oxygen where the levels were reduced. At 75 ^{o}C the development of the degradation product concentrations with time was more complex. HEA and OZD concentrations increased with time, BHEOX, HEF, HEPO and HEI levelled off whereas HEGly went through a maximum and then decreased. Laboratory reaction experiments were used to verify the formation of degradation products for some of the suggested mechanisms.

Acknowledgements
The work is done under the SOLVit project and the EU project OCTAVIUS FP7/295645. The SOLVit project is performed under the strategic Norwegian research program CLIMIT. The authors acknowledge the partners in SOLVit: Aker Clean Carbon, Gassnova, EON, EnBW and the Research Council of Norway for their support.

References

Bedell, S.A., 2009. Oxidative degradation mechanisms for amines in a flue gas capture. Energy Procedia 1, 771 - 778.
Bello, A., Idem, R.O., 2006. Comprehensive Study of the Kinetics of the Oxidative Degradation of CO_2 Loaded and Concentrated Aqueous Monoethanolamine (MEA) with and without Sodium Metavanadate during CO_2 Absorption from Flue Gases. Industrial & Engineering Chemistry Research 45, 2569-2579.
Ben, D.S.P., 2005. Process for the preparation of -1-(2-hydroxyethyl) imidazole, p. 6pp.
Blachly, C.H., Ravner, H., 1966. Stabilization of monoethanolamine solutions in carbon dioxide scrubbers. Journal of Chemical and Engineering Data 11, 401-403.
Chi, S., Rochelle, G.T., 2002. Oxidative degradation of monoethanolamine. Ind. Eng. Chem. Res. 41, 4178-4186.
Closmann, F., Rochelle, G.T., 2011. Degradation of aqueous methyldiethanolamine by temperature and oxygen cycling. Energy Procedia 4, 23-28.
da Silva, E.F., Lepaumier, H., Grimstvedt, A., Vevelstad, S.J., Einbu, A., Vernstad, K., Svendsen, H.F., Zahlsen, K., 2012. Understanding 2-Ethanolamine Degradation in Postcombustion CO_2 Capture. Industrial & Engineering Chemistry Research 51, 13329-13338.
Goff, G.S., Rochelle, G.T., 2004. Monoethanolamine Degradation: O_2 Mass Transfer Effects under CO_2 Capture Conditions. Industrial & Engineering Chemistry Research 43, 6400-6408.
Goff, G.S., Rochelle, G.T., 2006. Oxidation Inhibitors for Copper and Iron Catalyzed Degradation of Monoethanolamine in CO_2 Capture Processes. Industrial & Engineering Chemistry Research 45, 2513-2521.
Gouedard, C., Picq, D., Launay, F., Carrette, P.L., 2012. Amine degradation in CO_2 capture. I. A review. International Journal of Greenhouse Gas Control 10, 244-270.

Higgins, J., Zhou, X., Liu, R., Huang, T.T.S., 1997. Theoretical Study of Thermal Decomposition Mechanism of Oxalic Acid. The Journal of Physical Chemistry A 101, 2702-2708.
Huang, L., Li, L., Dong, W., Liu, Y., Hou, H., 2008. Removal of Ammonia by OH Radical in Aqueous Phase. Environmental Science & Technology 42, 8070-8075.
Hull, L.A., Davis, G.T., Rosenblatt, D.H., Williams, H.K.R., Weglein, R.C., 1967. Oxidations of amines. III. Duality of mechanims in the reaction of amines with chlorine dioxide. J. Am. Chem. Soc. 89, 8.
Hull, L.A., Giordano, D.H., Rosenblatt, D.H., Davis, G.T., Mann, C.K., Milliken, S.B., 1969. Oxidations of amines. VIII. Role of the cation radical in the oxidation of triethylenediamine by chlorine dioxide and hypochlorous acid. The Journal of Physical Chemistry 73, 6.
Katsuura, A., Washio, N., 2005. Preparation of imidazoles from imines and iminoacetaldehydes, p. 6 pp.
Kawasaki, N., Noguchi, Y., Aoki, H., Fujii, K., 1991. Preparation of 1-substituted imidazoles, p. 7 pp.
Kim, I., Svendsen, H.F., Børresen, E., 2008. Ebulliometric Determination of Vapor-Liquid Equilibria for Pure Water, Monoethanolamine, N-Methyldiethanolamine, 3-(Methylamino)-propylamine, and Their Binary and Ternary Solutions. Journal of Chemical & Engineering Data 53, 2521-2531.
Kjeldahl, J., 1883. A new method of determining nitrogen in organic substances. Zeits. Anal. Chem. 22, 366-382.
Kohl, A.L., Nielsen, R.B., 1997. Gas purification, 5 ed. Elsevier: Houston, TX, 1997.
Lawal, O., Bello, A., Idem, R., 2005. The Role of Methyl Diethanolamine (MDEA) in Preventing the Oxidative Degradation of CO_2 Loaded and Concentrated Aqueous Monoethanolamine (MEA)-MDEA Blends during CO_2 Absorption from Flue Gases. Industrial & Engineering Chemistry Research 44, 1874-1896.
Lepaumier, H., 2008. Étude des mecanismes de dégradation des amines utilisees pour le captage du CO_2 dans les fumées, Sciences Pour l'Ingénieur. Savoie.
Lepaumier, H., da Silva, E.F., Einbu, A., Grimstvedt, A., Knudsen, J.N., Zahlsen, K., Svendsen, H.F., 2011a. Comparison of MEA degradation in pilot-scale with lab-scale experiments. Energy Procedia 4, 1652-1659.
Lepaumier, H., Grimstvedt, A., Vernstad, K., Zahlsen, K.r., Svendsen, H.F., 2011b. Degradation of MMEA at absorber and stripper conditions. Chemical Engineering Science 66, 3491-3498.
Lepaumier, H., Picq, D., Carrette, P.-L., 2009. New Amines for CO_2 Capture. II. Oxidative Degradation Mechanisms. Industrial & Engineering Chemistry Research 48, 9068-9075.
Ma'mun, S., Svendsen, H.F., Hoff, K.A., Juliussen, O., 2007. Selection of new absorbents for carbon dioxide capture. Energy Conversion and Management 48, 251-258.
Patil, Y.P., Tambade, P.J., Jagtap, S.R., Bhanage, B.M., 2008. Synthesis of 2-oxazolidinones/2-imidazolidinones from CO_2, different epoxides and amino alcohols/alkylene diamines using Br-Ph3+P-PEG600-P+Ph3Br as homogenous recyclable catalyst. Journal of Molecular Catalysis A: Chemical 289, 14-21.
Prasanthi, V., Sivanadh, M., Rao, K.N., Rao, M.V.B., 2007. Convenient and improved one-pot synthesis of imidazole. Asian J. Chem. 19, 5778-5780.
Rooney, P.C., Dupart, M.S., Bacon, T.R., 1998. Oxygen's role in alkanolamine degradation. Hydrocarbon Process., 109 - 113.
Rosenblatt, D.H., Hull, L.A., De Luca, D.C., Davis, G.T., Weglein, R.C., 1967. Oxidations of amines. II. Substituents effects in chlorine dioxide oxidations. J. Am. Chem. Soc. 89, 6.
Sexton, A.J., 2008. Amine oxidation in CO_2 capture processes. The University of Texas, Austin, p. 262.

Sexton, A.J., Rochelle, G.T., 2009. Catalysts and inhibitors for oxidative degradation of monoethanolamine. International Journal of Greenhouse Gas Control 3, 704-711.
Sexton, A.J., Rochelle, G.T., 2011. Reaction Products from the Oxidative Degradation of Monoethanolamine. Industrial & Engineering Chemistry Research 50, 667-673.
Strazisar, B.R., Anderson, R.R., White, C.M., 2003. Degradation Pathways for Monoethanolamine in a CO_2 Capture Facility. Energy & Fuels 17, 1034-1039.
Supap, T., Idem, R., Tontiwachwuthikul, P., Saiwan, C., 2006. Analysis of Monoethanolamine and Its Oxidative Degradation Products during CO_2 Absorption from Flue Gases: A Comparative Study of GC-MS, HPLC-RID, and CE-DAD Analytical Techniques and Possible Optimum Combinations. Industrial & Engineering Chemistry Research 45, 2437-2451.
Supap, T., Idem, R., Tontiwachwuthikul, P., Saiwan, C., 2009. Kinetics of sulfur dioxide- and oxygen-induced degradation of aqueous monoethanolamine solution during CO2 absorption from power plant flue gas streams. International Journal of Greenhouse Gas Control 3, 133-142.
Supap, T., Idem, R., Veawab, A., Aroonwilas, A., Tontiwachwuthikul, P., Chakma, A., Kybett, B.D., 2001. Kinetics of the Oxidative Degradation of Aqueous Monoethanolamine in a Flue Gas Treating Unit. Industrial & Engineering Chemistry Research 40, 3445-3450.
Uyanga, I.J., Idem, R.O., 2007. Studies of SO_2- and O_2-Induced Degradation of Aqueous MEA during CO_2 Capture from Power Plant Flue Gas Streams. Industrial & Engineering Chemistry Research 46, 2558-2566.
Vevelstad, S.J., Grimstvedt, A., Knuutila, H., Svendsen, H.F., 2013. Thermal degradation on already oxidatively degraded solution. Submitted to Energy Procedia.
Wang, A., Edwards, J.G., Davies, J.A., 1994. Photooxidation of aqueous ammonia with titania-based heterogeneous catalysts. Sol. Energy 52, 459-466.
Wang, T., Jens, K.-J., 2011. A study of Oxidative Degradation of AMP for Post-combustion CO_2 Capture. Energy Procedia 23, 102-110.

Supporting information

Chemical stability – experiment using 6% O_2.

Oxidative degradation screening setup – experimental procedure

The Heidolph star-fish set-up is an apparatus for oxidative degradation experiments in open batch reactors. The set-up consists of 5 reactors in parallel, in principle a simplified version of the flow sheet given in Figure 1, but without pre-humidification and recycle of gas. The purpose of the experiments is screening of amines exposed to oxidative degradation. The set-up comprises five 250 mL three-necked round bottles which makes it possible to do 5 different experiments at the same time. MEA solution (100-150 mL), a priori loaded with CO_2 (0.4), was introduced into each of the round bottles. A metal mixture of $Fe(II)SO_4*7H_2O$ (0.4 mM Fe), $Cr(III)SO_4*xH_2O$ (0.1mM Cr) and $NiSO_4*6H_2O$ (0.05mM Ni) were added to each reactor. A dry gas blend of 2% CO_2, 6% O_2 and 94% N_2 was bubbled through the solution. The solutions were stirred and heated at 55 °C for 4 weeks. Liquid samples were taken out regularly and analysed for alkalinity using titration. All of the concentrations were adjusted according to the water balance (1-5 % loss).

Results

Amine concentration (mmol/L) corrected for water loss (1-5%) for the 5 reactors and the mean value for all reactors is given in table S.1.

Table S.1: Amine concentration (mmol/L) corrected for water loss (1-5%) for the 5 reactors and the mean value for all reactors.

Time (hours)	Amine concentration (mmol/L)					
	R1	R2	R3	R4	R5	Mean
0	4400	4450	4510	4390	4490	4448
24	3329	4432	4412	4398	4443	4203
96	4282	4397	4378	4333	4343	4347
192	4245	4345	4317	4266	4286	4292
312	4246	4236	4267	4228	4253	4246
504	4211	4086	4146	4184	4170	4159
600	4193	4007	4096	4138	4134	4114

The screening setup has to go through more tests before base case is established. The data is therefore only estimates and mean values are used. In table S.2 degradation rate (mM/h) is given where mean value for R2-R4 is used in Figure 3.

Table S.2: Degradation rate (mM/h) for the 5 different reactors and the mean value.

	Degradation rate (mM/h)
R1	-0.40
R2	0.74
R3	0.61
R4	0.42
R5	0.54
Mean R2-R5	0.58

Nitrogen balance

Overall nitrogen balance

Overall nitrogen balance was calculated from measured organic nitrogen in liquid phase end sample (Kjeldahl method, mol) and initial MEA (mol). Amount of organic nitrogen in end sample was adjusted according to water balance.

Table S.3: Overall nitrogen balance

T (°C)	Oxygen (%)	Org N in liquid phase (%)
55	21	94
55	21	93
55	50	91
55	98	89
75	21	78

Gas bubble flasks

Exit gas was bubbled through water for MEA experiment run 1 and experiment at 75 °C. The end sample from gas bubble flask from MEA experiment 1 and experiment at 75 °C were analysed and quantified for MEA and LC-MS mix. The volume of water is estimated with a minimum (min, ~50 mL) and maximum (max, ~150 mL) value and the amount of each analyte is found at miniumum and maixmum water volume in gas bottle flask is compared toward the same analyte (mmol) in the solvent end sample as shown in table S.4 for the analytes from the LC-MS mix for MEA experiment run 1 at 55 °C and in table S.5 for the MEA experiment at 75 °C.

Table S.4: Amount of analyte (mmol) in gas bubble flask estimated based on minimum and maximum water volume together with amount of analyte in the end solvent sample for the MEA experiment run 1.

Analyte (mmol)	Max (gas bubble flask)	Min (gas bubble flask)	Solvent (end)
OZD	7.3E-04	2.8E-04	3.9
BHEOX	5.0E-05	1.9E-05	1.5
HEA	3.0E-04	1.1E-04	0.7
HEGly	1.7E-03	6.5E-04	7.3
HEPO	1.2E-05	4.4E-06	0.6
HEF	8.7E-03	8.7E-03	21.5
HEI	1.9E-03	7.1E-04	2.3

Table S.5: Amount of analyte (mmol) in gas bubble flask estimated based on minimum and maixumim water volume together with amount of analyte in the end solvent sample for MEA experiment at 75 °C.

Analyte (mmol)	Max (gas bubble flask)	Min (gas bubble flask)	Solvent (end)
OZD	6.4E-03	2.4E-03	10.9
BHEOX	6.3E-04	2.4E-04	1.6
HEA	4.5E-03	1.7E-03	8.8
HEGly	5.3E-03	2.0E-03	9.7
HEPO	0E+00	0E+00	3.7
HEF	2.3E-01	8.7E-02	37.2
HEI	2.5E-02	9.5E-03	18.2

MEA (mmol) in initial and end solvent sample and in gas outlet for minimum and maximum values are given in table S6.

Table S.6: MEA (mmol) in solvent (initial and end) and gas outlet (max and min).

Experiment	Solvent - MEA (mmol)		Gas outlet (end) - MEA (mmol)	
	Initial	End	Max	Min
21% O_2 55C	4898	3972	1.92	0.72
21% O_2 75C	4898	1997	18.21	6.86

GC-MS scan degradation compounds (method described by Lepaumier (Lepaumier et al., 2011b)

Analysis of end sample for experiment 21% O_2 run1

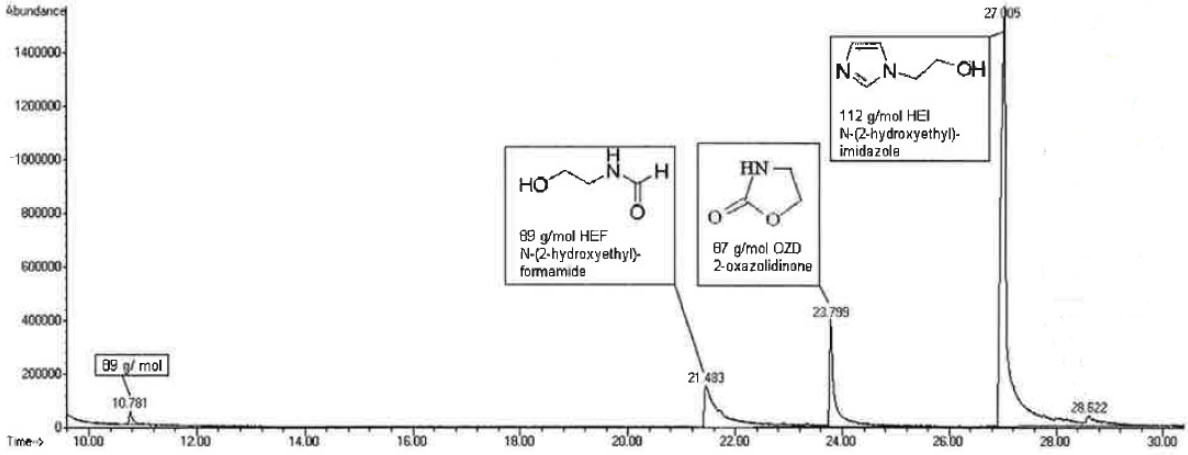

Figure S.1: End sample MEA run 1, dilution 1/10, analysed using Chemical Ionisation (CI) scan mode.

Peak 1:
Retention time: 10.8 min
Molecular weight: 89 g/mol
Compound: Unknown

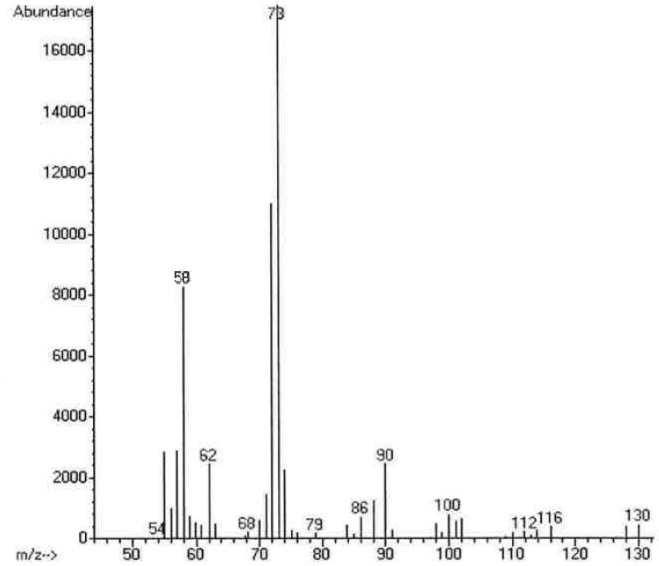

Figure S.2: Mass spectrum for peak 1.

Peak 2:
Retention time: 21.5 min
Molecular weight: 89 g/mol

Compound: *N*-(2-hydroxyethyl)formamide (HEF):

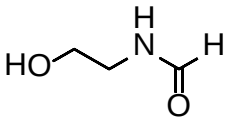

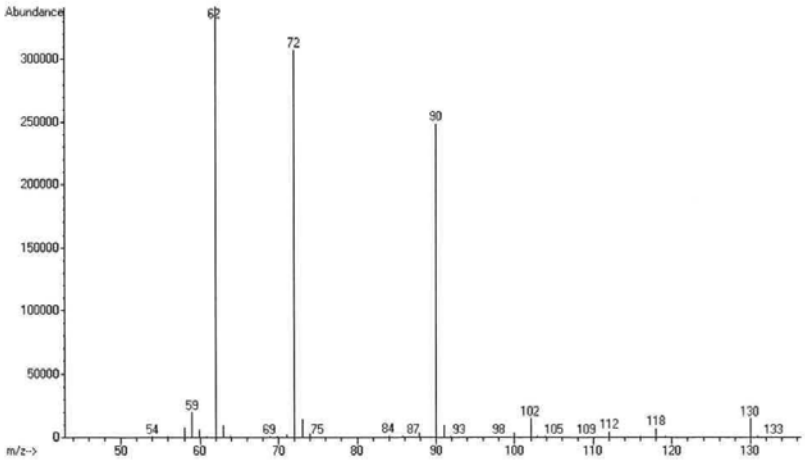

Figure S.3: Mass spectrum for peak 2.

Peak 3:
Retention time: 23.8 min
Molecular weight: 87 g/mol

Compound: 2-Oxazolidinone (OZD):

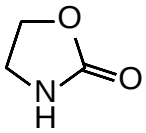

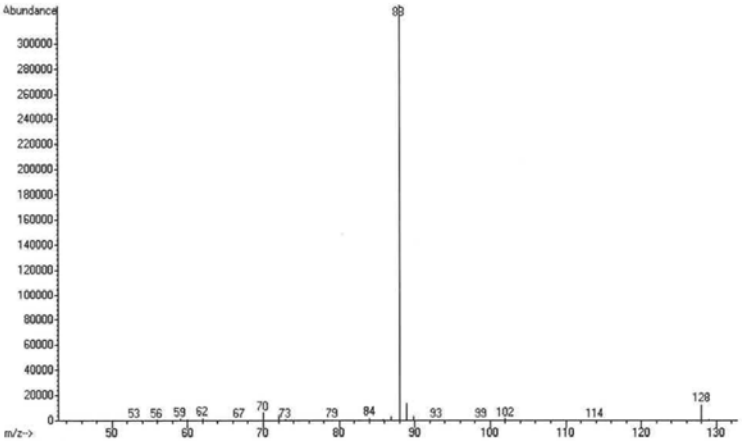

Figure S.4: Mass spectrum for peak 3.

Peak 4:
Retention time: 27.0 min
Molecular weight: 112 g/mol

Compound: *N*-(2-hydroxyethyl)-imidazole (HEI): 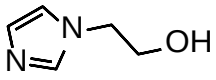

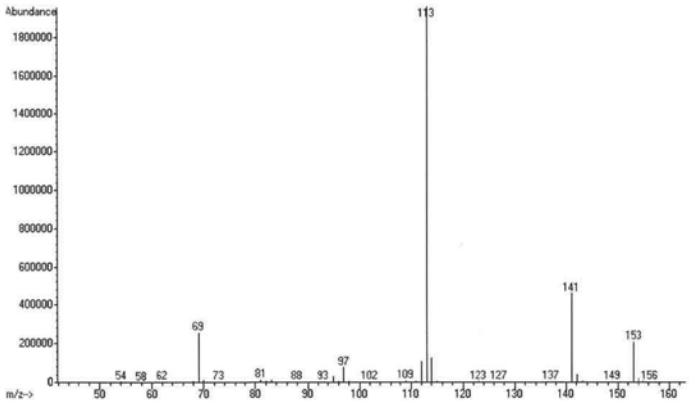

Figure S.5: Mass spectrum for peak 4.

Peak 5:
Retention time: 28.6 min
Molecular weight: 126 g/mol

Compound: 2-methyl-1H-imidazole-1-ethanol (1615-15-2): 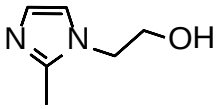

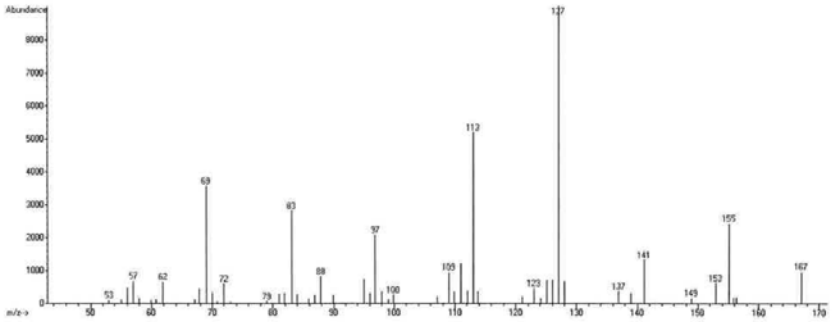

Figure S.6: Mass spectrum for peak 5.

Uncertainty calculations

Nitrogen recovery (table 2)

The Nitrogen recovery R_N may be expressed as :

$$R_N = \frac{\sum \vartheta_j C_j}{W_N \rho} = \frac{C_{MEA}}{W_N \rho} + \frac{\sum \vartheta_i C_{Deg,i}}{W_N \rho}$$

Her C is concentrations in mol/l, W_N is nitrogen in mol/kg, ρ is density and v is stoichiometric coefficient for number of nitrogen per molecule.

The uncertainty in R_N may be obtained from a combination of the analytical uncertainties and could be expressed by the law of error propagation as :

$$\Delta R_N = \sqrt{\left(\frac{\partial R_N}{\partial C_{MEA}}\right)^2 \Delta C_{MEA}^2 + \left(\frac{\partial R_N}{\partial W_N}\right)^2 \Delta W_N^2 + \left(\frac{\partial R_N}{\partial \rho}\right)^2 \Delta \rho^2 + \sum \left(\frac{\partial R_N}{\partial C_{Deg,i}}\right)^2 \Delta C_{Deg,i}^2}$$

As the value of the last term is neglectable (i.e. absolute uncertainty of degradation concentrations << uncertainty of MEA) compared to the other terms the expression can be reduced to:

$$\Delta R_N \approx \sqrt{\left(\frac{1}{W_N \times \rho}\right)^2 \Delta C_{MEA}^2 + \left(\frac{\rho \times C_{MEA}}{(W_N \times \rho)^2}\right)^2 \Delta W_N^2 + \left(\frac{C_{MEA} \times W_N}{(W_N \times \rho)^2}\right)^2 \Delta \rho^2}$$

By using the data for the 21%O_2 experiment and 5% relative uncertainty for MEA, 2 % relative for the nitrogen and 0.5% relative for the density the combined uncertainty for R_N becomes:

$$\Delta R_N \approx \sqrt{\left(\frac{1}{4.44}\right)^2 \times 0.21 + \left(\frac{1.0908 \times 4.19}{(4.44)^2}\right)^2 \times 0.081 + \left(\frac{4.19 \times 4.44}{(4.44)^2}\right)^2 \times 0.055}$$

This shows that the uncertainty in the nitrogen recovery (or N balance) is around 5%.